**LIGHTWEIGHT STRUCTURES in CIVIL ENGINEERING**
**CONTEMPORARY PROBLEMS**
Monograph from Scientific Seminar
Organized by Polish Chapters of
**International Association for Shell and Spatial Structures**
Lodz University of Technology
Faculty of Civil Engineering, Architecture and Environmental Engineering
**XXIV LSCE**
**Łódź, 7th of December 2018 (Friday)**

# PROBABILISTIC METHODS IN RELIABILITY ASSESSMENT OF ENGINEERING LIGHTWEIGHT STRUCTURES

**K. Winkelmann** [1)]
[1)] PhD, Faculty of Civil and Environmental Engineering, Gdańsk University of Technology, POLAND, *karolwin@pg.edu.pl*

**ABSTRACT:** The paper considers the probability-based analysis of structural safety measures. Two different numerical examples of representative lightweight structures are considered – a submerged truss tower supporting an offshore platform, and an overhead power line support truss tower. On the basis of these examples, the importance of a motivated selection of analysis method and a proper choice of the number of important variables is shown. Moreover, formulation of the reliability index related to the response of a considered structure is presented, alongside the possibility of adjusting the random methodology to the given task. The structures under consideration are burdened with uncertainties – material and load imperfections. Additionally, the simulation is performed of the impact of chosen imperfections to the structural reliability decrement in the time of structural service. Such an applicability overview of random methodology is performed to show that even a diverse structural domain may be analysed by a versatile random approach. Moreover, proper reliability estimation is possible even for specifically simplified cases.

**Keywords:** reliability, sensitivity, lightweight structures, material and geometric imperfections, variable load

## 1. INTRODUCTION

In present day, considering engineering randomness is the standard routine in the design process, moreover, it is a field of continuous development.

The standard approach to randomness is in fact deterministic, the so-called Level 1 approach. Load and structural uncertainties are included in the design in the form of total or partial load and resistance safety factors set in the design codes (Ref. 1). However, the factors may be subjected to further user-oriented calibration. Factor-based design is the basis of probabilistic codes, e.g. the regulations provided by the Joint Committee on Structural Safety (JCSS) in the Probabilistic Model Code (Ref. 2). Due to the Level 1 assumptions structural reliability tends to capture full complexity of real-life engineering structures, the impact of its uncertainty to structural response parameters, however it specifies random parameters only in the form of certain numerical data determined on the basis of engineering experience and practice, as shown in Ref. 3.

In the design processes of key importance structures, higher level methods are introduced, with a tendency towards a full probabilistic approach.

The Level 2 methods of structural safety assessment regard probabilistic nature of the problem by means of two probabilistic moments per each variable considered: its mean value and variance, in most cases supplemented by the measure of correlation between these parameters. These methods are often identified with a simplified representation of the failure region, introducing simple and straightforward safety measures (Ref. 4).

The Level 3 methods, do not include any simplifying algorithms, instead they use a full probabilistic description of the phenomena. They mainly focus on providing a broad description of structural failure, based on spatial integration of multivariate cumulative probability density functions of the considered random variables. Regardless of the applied probability-based approach level, reliability estimated on the basis of the methods is often expressed by means of strict structural safety measures, e.g. failure probability or reliability indices (Ref. 5).

It is worth noting, that each individual structural factor, such as the type, size, importance of the structure and the assumed number of basic variables related to load and material uncertainties affects the reliability measures (Ref. 6). While properly assessed, the approach is mostly focused on assuring an anticipated reliability level of an analysed structure.

Numerous computational methods are strictly aimed at reliability assessment. Nevertheless, the classification of probabilistic methods, techniques and theories is difficult to perform. It is usually executed with regard to the required final analytical results, or the undertaken solution path (Refs 7 - 20).

Unfortunately, there does not exist a clearly defined recommendation of the reliability assessment method due to a given engineering problem class. The ability to match the probabilistic approach to the problem in order to minimize its numerical effort, whilst aiming at proper estimation of failure probability is a key issue in reliability analysis.

Nowadays, due to the development of computer-aided design tools, civil engineering finds the crude Monte Carlo method dominant and widespread, due to the ability of swift repetitive computations (Refs 21 - 26). Moreover, effectiveness problems of the Monte Carlo methods (time consumption and slow convergence) are further solved by means of variance reduction techniques. The most popular techniques of this domain are: Stratified Sampling (SS), Importance Sampling (IS), Adaptive Sampling (AS), Latin Hypercube Sampling (LHS) or Targeted Random Sampling (TRS) (Ref. 24)

Other methods, such as the Point Estimate Method (PEM) (Ref. 27), Mean Value First Order (MVFO) (Ref. 10), First and Second Order Reliability Methods (FORM, SORM) (Refs 5, 28 - 30), Perturbation Method (Refs 6, 18, 31) or Genetic Algorithms (GA) (Ref. 19) are commonly used to properly assess the expected reliability level.

The Response Surface Method (RSM) is an effective tool to analyse structural response to various actions (Refs 6, 18, 32). The RSM either explores simple techniques listed above to solely assess reliability indices assessment or to perform the response approximation task in combination with specific associated approaches, such as the MC method (Ref. 33).

In a more complex stochastic analysis it is necessary to deal with time-space variable processes. In these cases the Stochastic Finite Element Method (SFEM) is incorporated to consider structural responses to random time- and/or space-dependent processes (Refs 19, 34 - 36).

## 2. AIM OF THE STUDY

In general structural reliability is strongly affected by uncertainty parameters decisive in the problem, the so-called basic variables. Uncertainty in structural systems may take its origin in material imperfections (e.g. corrosion), geometric imperfections, load variability (e.g. wind, snow, icing) and load return period (e.g. excessive winds, high waves). Moreover, reliability index in selected cases is strongly time-variant, triggering the need of stochastic analysis or an equivalent set of time-invariant computational scenarios.

The paper shows the importance of motivated selection of an appropriate analytical method to estimate the reliability of engineering structures subjected to uncertain means. The examples are shown to present a possible method to properly assess the number of variables, based on a deterministic sensitivity analysis. They also lead to the choice of reliability index form, based on the size of the random vector of the task and the predicted structural response.

Moreover, the paper simulates the impact of structural element degradation due to external factors to the decrement of structural reliability in structural service time.

The analysis is performed on two representative lightweight structures. The paper concerns a submerged truss tower supporting an offshore platform, presented in Ref. 37 and an overhead power line support truss tower, introduced in Refs 38, 39.

## 3. SENSITIVITY AND RELIABILITY ASSESSMENT OF A SUBMERGED TRUSS TOWER SUPPORING AN OFFSHORE WIND POWER PLANT CONSIDERING TIME-VARIANT MATERIAL DEGRADATION

A three-dimensional truss-like tower is considered (Fig. 1), creating a semi – submerged support for an offshore platform – an oceanic wind power plant. The structural model is presented in Ref. 37.

### 3.1. Details of tower geometry and material used

The tower structure of a total 66 m height is divided into four segments of varied heights. The top 12 m (segment 1) is above the natural sea water level and the bottom 15+18+21 = 54 m (segments 2 – 4) lie beneath the surface. The structural parts are a square frustum of a constant convergence of 6%. The base side of the square varies from ca. 12 m to ca. 6 m.

All structural elements (legs and stiffeners) are made of circular hollow profiles. Segments 1 – 3 (legs) show a 1.15 m diameter and 30 mm thickness, segment 4 (legs) shows a 1.30 m diameter and 55 mm thickness, the bracings show a 0.73 m diameter and 20 mm thickness. The vertical stiffeners form a diagonal X-truss pattern, no horizontal stiffeners are included. The numerical model employs technological connection of the segments – it assumes semi-rigid connector elements, each 2.00 m high, made of circular hollow profiles of a 1.28 m diameter and 43 mm thickness.

All elements of the tower are made of high-class structural steel of a $f_y$ = 345 MPa yield limit, modulus of elasticity $E$ = 210 GPa, Poisson's ratio $\upsilon$ = 0.3, and mass density $\rho$ = 8500 kg/m$^3$.

The structure was modelled in Simulia ABAQUS/CAE 6.14-2. The elements were modelled as B31 bi-nodal beam elements of a vertical length of 1 m. The pin-joints were modelled as quasi-rigid.

### 3.2. Structural loads

The tower was loaded with a typical set of loads, adjusted to offshore platforms for wind power plants. The concrete deck slab dead load, the total mass of power plant structure with additional installations, wind load of both power mill and segment 1 and wave hydrostatic and hydrodynamic pressure on segments 2 – 4 calculated according to Ref. 40 were considered.

The forces were represented as resultant forces acting on the respective nodes and elements of the structure.

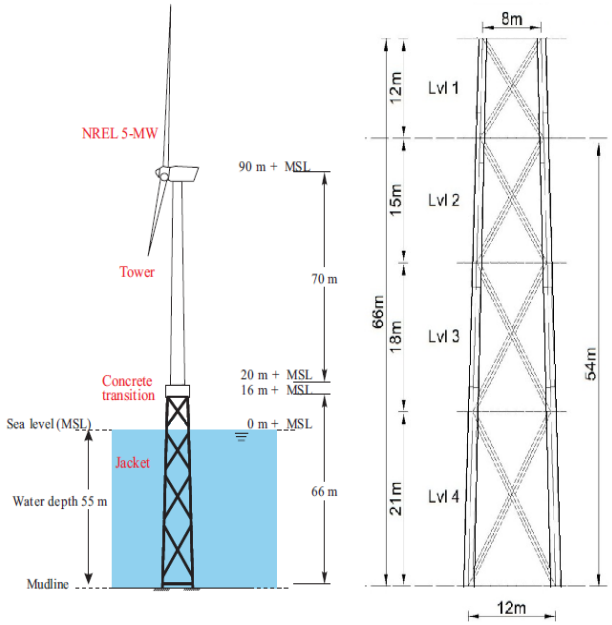


Fig. 1 An overview of the semi – submerged truss support tower of an oceanic wind power plant (Ref. 37)

### 3.3. Objective of the analysis

The primary analytical goal of the semi-submerged truss support tower is to present a motivated choice of basic variables detecting the highest impact on structural behavior. Afterwards, a properly simplified probabilistic problem is analyzed in terms of reliability assessment, using standard computational techniques.

Finally, reliability is also assessed in set time-steps after 20 and 50 years of full service in oceanic conditions.

### 3.4. Definition of basic task variables and structural response

The tower is divided into four segments, each segment consists of both columns and struts of various cross-sectional parameters. The assumption was made to incorporate eight random variables in the task, connected with these presented groups of elements.

#### 3.4.1. Material degradation random variable

Each variable is bound to reflect Young's modulus variability, representing material parameter imperfection, due to electrochemical corrosion induced by constant exposition to salt water. This phenomenon was assumed a probabilistic model proposed by Weibull (Ref. 41). The Weibull probability density distribution is one-sided and continuous, thus it fits the variable parameters not exceeding a predetermined value. The initial Young's modulus of steel equal 210 GPa in this case (no strengthening possible).

The Weibull probability density function (PDF) is expressed using Eqn. 1 (Ref. 41):

$$f_X(x,\lambda,k)=\begin{cases}\dfrac{k}{\lambda}\left(\dfrac{x}{\lambda}\right)^{k-1}\exp^{-\left(\frac{x}{\lambda}\right)^k} & for\ x\geq 0\\ 0 & for\ x<0\end{cases} \tag{1}$$

where $k > 0$ is the shape parameter and $\lambda > 0$ is the scale parameter.

It is worth noting that the probability density function given by Eqn. 1 may not fit the elastic modulus variable well, setting the minimum value to zero while leaving the maximum infinite. Thus it was decided that the Weibull-type random variable is taken to express the modulus deterioration instead. Hence the real modulus is a determined by a difference, using the nominal modulus value, stated in Eqn. 2:

$$E_i = 210\,\text{GPa} - f_i(x,\lambda,k) \tag{2}$$

The Eqn. 2 form may, in turn, lead to an output value $f_i(x,\lambda,k) > 210$, inconsistent with the Young's modulus non-negative definition. However, due to a remote probability (< 0.0001) of such a generated value, it is automatically rejected if obtained.

### 3.4.2. Structural response definition

The observed structural response $u(x)$ was expressed in terms of critical load value multiplier, corresponding in every case to a randomly generated model in Simulia ABAQUS/CAE 6.14-2.

### 3.5. Deterministic sensitivity analysis of the tower in the scenario of material degradation

In the first analytical step, global structural sensitivity was assessed due to degradation of a given tower element.

In order to complete this step the change (deterioration) of Young's modulus was accepted as a discrete variable. The maximum modulus reduction was adopted as 60 GPa, the reductive step was taken as 10 GPa.

The graphs shown in Fig. 2 and in Fig. 3 present the influence of the steel degradation of a given element group on load-bearing capacity of the entire structure.

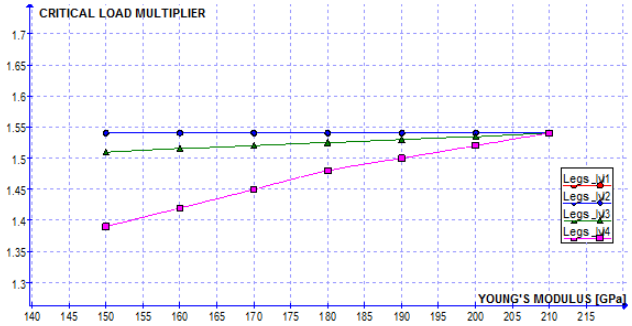


Fig. 2 The correlation between the material degradation (reduction of the elastic modulus of steel) of the truss legs and tower load capacity

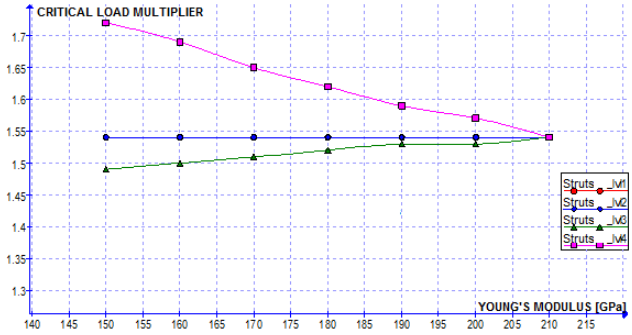


Fig. 3 The correlation between the material degradation (reduction of the elastic modulus of steel) of the struts and tower load capacity

Based on a preliminary sensitivity analysis it was shown that two random variables are decisive to the structural response only – the Young's modulus deterioration in legs of segment 4 of the submerged tower ($\Delta E_{L4}$) and the elastic modulus decrement in segment 3 struts ($\Delta E_{S3}$). Moreover, it was proved, that the combination of deterioration of both elements further reduces the load-carrying capacity of the tower, however this effect is not a simple superposition of both capacity reductions acting separately, a fact that is presented in Fig. 4.

It should be noted, that this additional analysis allows for sensitivity indices calculation, whereas at the same time an expected reliability level may be predicted.

While extrapolating (or approximating) the response with a proper order polynomial (linear is almost sufficient in the presented case), the critical load multiplier reaches the limit value of 1.0 in the case of marginally low values of elastic moduli (ca. 40 GPa). However, the studies of Ref. 37 show, that such a progressive corrosion is possible.

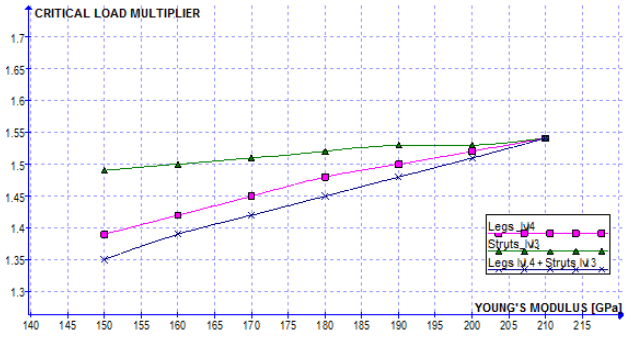


Fig. 4. The correlation between the material degradation of steel of both legs and struts and tower load capacity.

### 3.6. Reliability assessment of the tower in set time-steps after 20 and 50 years of full oceanic service

As determined in the previous chapter, the probabilistic problem may be simplified to a bi-variate task, as only two variables present a noticeable unfavorable effect on the load-carrying capacity of the submerged structure.

Two scenarios were considered – the structure analyzed after 20 and 50 years of full service in the desired oceanic conditions, assuming no defensive anti-corrosion installations on the tower.

### 3.6.1. Determination of the limit state function

In order to determine the allowable variability range of Young's modulus as a function of a joint probability density of both random variables of the task, it was decided to carry out a preliminary analysis to determine the limit state function (LSF). The LSF marks the region of correspondingly low Young's moduli to cause the critical coefficient lower than $\lambda = 1.0$, thus exceeding the load capacity of the structure.

In order to conduct the analysis, an OAT (One-At-A-Time) approach was assumed, determining a maximum discrete reduction of Young's modulus due to one random variable while maintaining a set discrete Young's modulus reduction for the second random variable. In other words, the structure exhibits a critical coefficient value for variable loads, equal $\lambda = 1.0$.

Sixteen different computational situations were analyzed, assuming the variability of the Young's modulus degradation every 10 GPa. Based on the analyzed calculations, the limit state function was performed, the results are presented in Fig. 5.

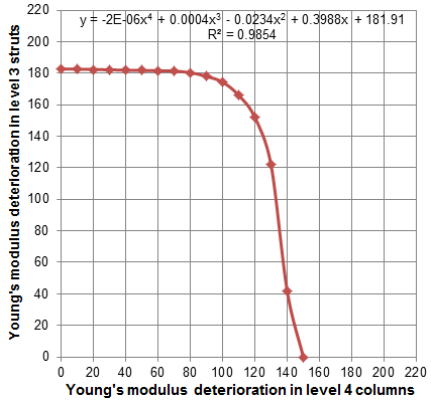


Fig. 5 The Limit State Function (4rd order polynomial approximation equation provided) of possible Young's moduli deterioration – the right hand side depicts the failure region

### 3.6.2. The choice of probabilistic methods

Based on the observations on the reliability performed in the preliminary sensitivity assessment, a relevant reliability estimation method should be chosen. In nominal cases reliability is relatively high, so the techniques to precisely deal with the Limit State Equation (LSE) are required.

In high-reliability cases the reference crude Monte Carlo method requires a great amount of processed samples. This may be problematic if a sample computation is equivalent to generation and non-linear numerical computations.
Hence, dedicated variance-reduction techniques are suggested - the Importance Sampling or the Targeted Random Sampling. The latter technique was applied in the paper.
While the structural response identified in the sensitivity analysis is quasi-linear, a good approximation of the response is possible, so the Response Surface Method should also generate a reliability index with a good compliance to the MC-based index. The RSM-based index was applied in the analysis too.
Due to a high numerical cost and a considerable time consumption of the computations, an amount of 50 random samples was generated due to each time-step scenario only.

### 3.6.1. The 20-year material degradation numerical case

In the 20-years simulation, the $k$ = 2.0 shape factor and $\lambda$ = 40.0 scale factor were used in the Eqn. 1. Such values were adopted a priori, however, the resultant probability density function obtained was similar to the one based on the observations included in Ref. 42. The image of the output Weibull probability density function is given in Fig. 6.

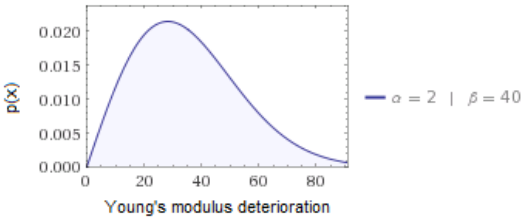


Fig. 6 The Weibull's probability density function of the Young's modulus degradation for the 20-years simulation

The results of the Monte Carlo method analysis for the 20-year scenario are presented in Fig. 7.
As shown in Fig. 7, in the 20-year scenario none of the MC points exceeds the limit state boundary, indicated in red. Thus the MC-based probability of failure is marked as zero, but this result is clearly wrong. This confirms the need of a far greater number of samples calculated in a high-reliability case (low probability of failure).
Given a number of 50 samples (in fact, even a smaller number of 20 samples) the approximation of the response surface slope factors is proved convergent, the RSM is proved to assess the reliability properly. The Hasofer – Lind index is $\beta_{HL,20years}$ = 3.54, corresponding to probability of failure of $P_{F,20years} = 0.2\times10^{-3}$. Similar results are provided by Targeted Random Sampling, however it should be noted that this technique requires the calculation of the next 50 samples and a dedicated software to determine the required samples.

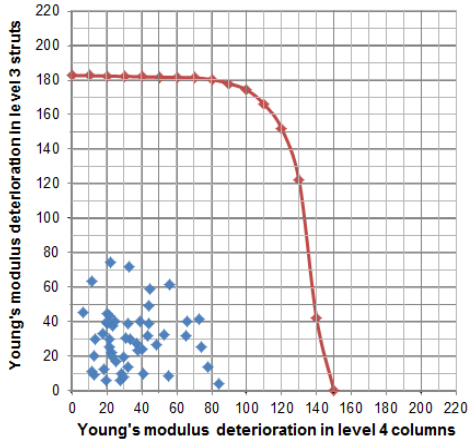


Fig. 7 The results of MC-based analysis for the advanced time scenarios – assuming 20 years of tower's full service in the oceanic conditions

### 3.6.2. The 50-year material degradation numerical case

Similarly, in the 50-years simulation the $k$ = 2.0 shape factor and $\lambda$ = 100.0 scale factor were used in the Eqn. 1, based on [42]. The image of the output Weibull probability density function (PDF) is given in Fig. 8. The sample draw from the latter PDF led to the rejection of samples with $E < 0$, so an additional computational error of generation was performed.
The results of the Monte Carlo method analysis for the 50-year scenario are presented in Fig. 9.

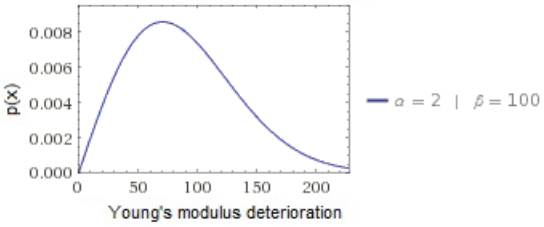


Fig. 8 The Weibull's probability density function of the Young's modulus degradation for the 50-years simulation

In the 50 year scenario the MC samples indicate a significantly higher probability of failure, equal to $P_{F,50years}$ = 0.2. This, in turn, corresponds to the reliability index of $\beta_{MC,20years}$ = 0.84.
A corresponding RSM approximation was also performed. It indicated that the reliability index is equal to $\beta_{HL,20years}$ = 0.91, the equivalent probability of failure equal to $P_{F,50years}$ = 0.181.
As it may be observed, this time the MC method result is supported by RSM. This is caused by the deteriorated case, hence reliability is considerably low. In such a strong dispersed cloud of Monte Carlo samples, see Fig. 9, it is easy for the limited set of samples to map the reliability correctly. Still, the number is low and the result is sensitive to the sample draw. Such a good agreement is accidental, yet its occurrence proves the conclusions of the analysis.
This time the equal-probability variant of Stratified Sampling technique, meant for big values of failure probability was used as a cross-check method. Although it requires the computation of 49 (7×7) new samples and a dedicated software to determine the samples, the method presents similar results.

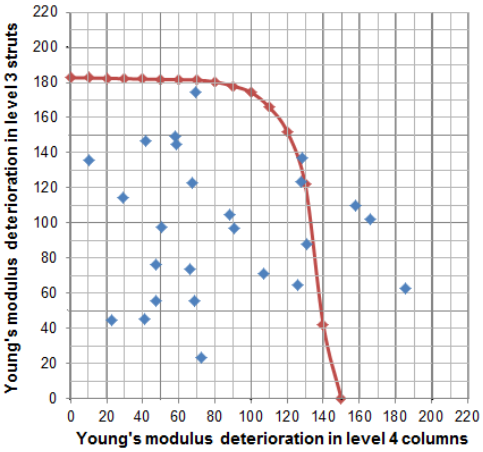


Fig. 9 The results of MC-based analysis for the advanced time scenarios – assuming 50 years of tower's full service in the oceanic conditions

### 3.6.3. The reliability variability during the material degradation

The results presented in the previous subchapters may be formulated in a closed-form function of the failure probability change due to the progressive material degradation. In order to perform this operation the RSM calculations results were applied. The function is presented in Fig. 10. The $P_F$ values are also given, moreover, quadratic approximation of the function of $P_F$ change is displayed.

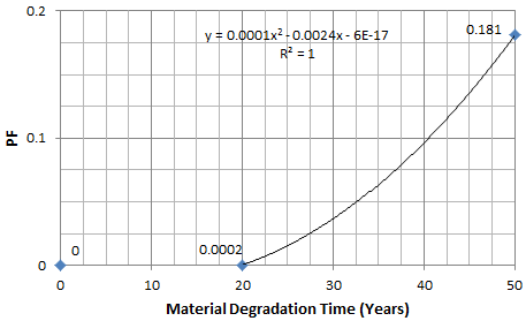


Fig. 10 The probability of failure results obtained using the Response Surface Method for different time scenarios

### 3.7. Remarks on the example

The results of both scenarios show, that the failure probabilities unacceptable for the engineers may be easily induced after ca. 20 years. Since the design life of a submerged structure may reach 100 years (although, several in-situ investigations with emergency repairs are performed during that time), such results indicate clearly, that providing effective anti-corrosion installations is required.

This way, reliability of the submerged tower may not be estimated high, even though the offshore structures are designed in an overly safe manner, as stated in Ref. 43.

On the other hand, every submerged structure is properly protected with paint coatings and cathodic protectors, which may imply a change in the degradation speed, not investigated in this paper. Parallel analysis should be initiated, taking into account the quality and efficiency of external protective installations in the reliability assessment.

An interesting fact is observed in the almost-symmetrical nature of the limit state function. This implies, that a failure may be triggered in almost equal measures by only the segment 4 columns degradation, as it could be triggered by the material deterioration of the segment 3 struts.

Moreover, the stiffening effect of the support in the bedrock, responsible for the transfer of a certain level of internal load from struts of segment 4 to the legs of segment 4, explains why the reduction of the before mentioned struts elastic modulus acts positively on the structure.

## 4. SENSITIVITY AND RELIABILITY ASSESSMENT OF AN OVERHEAD POWER LINE SUPPORT TRUSS TOWER CONSIDERING THE LOAD RETURN PERIOD

A three-dimensional truss-like tower is considered (Fig. 11), constituting a support structure for an overhead power line, an element of the electrical grid infrastructure. The model of the structure was provided by the SAG Elbud Gdańsk design office. The model was previously analyzed by the Author in Refs 38 and 39.

### 4.1. Details of tower geometry and material used

The total height of the OS24 ON150+10 tower is 32.15 m. The lower structural part (the segments below 22 m) is a pyramid frustum of a constant convergence of 12.15%. The base side of a pyramid varies from 7.03 to 1.68 m. The upper structural part (segments from 22 to 32.15 m) form a prism whose side length is 1.68 m.

In the upper part of the tower, eight lateral truss cross-arms are situated, they are loaded by six AFL-6 240 phase wires (conductors) with $f_u$ = 83.4 MPa and two AFL-1.7 70 earthed wires with $f_u$ = 160.0 MPa. The span between adjacent towers equals 280 m.

All structural elements (columns and stiffeners) are made of hot rolled identical angle sections whose dimensions range from 35×4 to 120×10. Both vertical and horizontal stiffeners form a diagonal X-truss pattern.

The numerical model assumes fully rigid connections between elements at all structural nodes.

All elements of the tower are made of St3S structural steel of a yield limit $f_y$ = 215 MPa, tensile strength $f_u$ = 375 MPa, modulus of elasticity $E$ = 205 GPa, shear modulus $G$ = 80 GPa, Poisson's ratio $\upsilon$ = 0.3 and mass density of $\rho$ = 7700 kg/m$^3$.

The structure was modelled in Autodesk ROBOT Structural Analysis Professional 2016 commercial software. Beam elements were chosen in the task. The support nodes were modelled as pin-joints, according to real-life structural model.

### 4.2. Structural loads considered

The tower was loaded with a typical set of 16 various loads, encapsulating the dead loads, assembler and wire loads, wind and icing acting on the wires, wind acting on each side of the tower, standard wire pre-tensioning and the wire-snap failure cases.

All the loads were considered as resultant forces acting on respective structural nodes and elements.

Afterwards, 16 extreme load combinations were proposed, to model real tower loading in limit cases. The Ultimate Limit State (ULS) investigation was planned, both stability loss and plastic failures were observed in different elements in various load combinations. The failure mostly occurred in the cross-bars (plastic failure) or in the curbs situated in the vicinity of supports (stability loss).

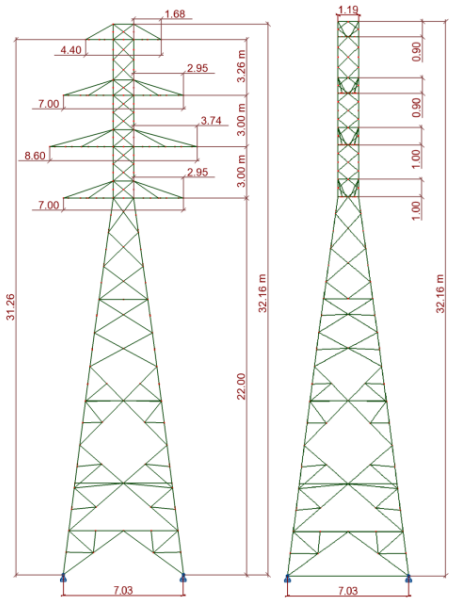


Fig. 11 An overview of the OS24 ON150+10 support tower of an overhead power line (Refs 38, 39).

### 4.3. Objective of the analysis

First of all, in the analysis of the support tower, a relevant probabilistic modelling of two climate loads (wind and icing) is assessed. Their joint action is considered, so their resultant sum-of-load action on the structure itself is investigated.

The considered probabilistic problem is analyzed in terms of reliability assessment for both elements mentioned before, applying standard computational techniques.

Finally, reliability is also assessed in connection with a return time period – after 50, 150 and 500 years.

### 4.4. Definition of the task variables and structural response

The sensitivity analysis for the considered tower, similar to the one presented in Chapter 3, was performed earlier by the Author, in Ref. 38.

In the paper, the focus of the analysis is transferred to the response change observation for the variable atmospheric load. Random description of wind and icing load is presented.

#### 4.4.1. Probabilistic wind load

Probabilistic model of the wind load incorporates the Gumbel variable (Extreme Type I), commonly used to model these load types, see Ref. 44. The experimental data to assess the distribution parameters were based on Gdynia Airport measurements consisting of maximum monthly wind speed data from a period of three years.

The cumulative distribution function of the Gumbel variable is given by Eqn. 3 (Ref. 45):

$$f_X(x,\alpha,\beta) = \alpha \cdot \exp\left\{-\alpha(x-\beta) - \exp\left[-\alpha(x-\beta)\right]\right\} \quad (3)$$

where $\alpha$ is the location parameter and $\beta > 0$ is the scale parameter.
In order to determine the Gumbel-type variable parameters, the basic procedure explained in [46] has been used. The parameters for Eqn. 3, obtained for the averaged maximum winds are: α = 2.875, β = 10.348.
The image of the Gumbel probability density function (PDF) is presented in Fig. 12.

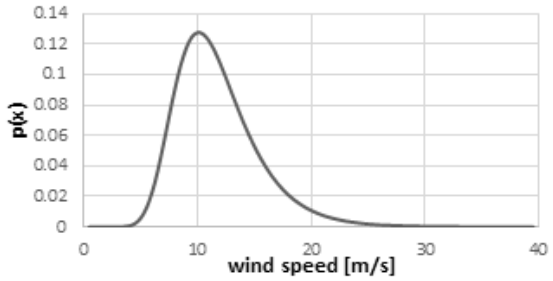


Fig. 12 The Gumbel's probability density function of the maximum monthly wind load (in terms of the wind speed)

The distribution covers an entire real numbers domain (□), thus a bounded Gumbel PDF is a proper solution, yet due to the marginal generation probability (< 0.0001) of a negative or enormously high value both cases are automatically rejected with minimal generation error.
Apart from the descriptions given above, the wind load return period is also taken into account, as three different time scenarios are analyzed. The resulting return periods, both in months and years, for each wind velocity in m/s is presented in Fig. 13.

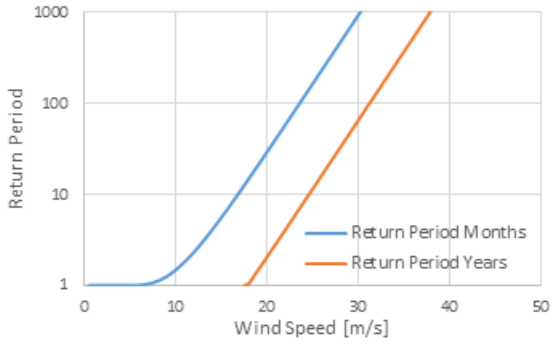


Fig. 13. Return period for probabilistic wind load speed

The assumed failure mode is associated with the mean wind velocity. The relation between the mean value of wind and the wind velocity for each section of the considered tower is shown in Fig. 14.

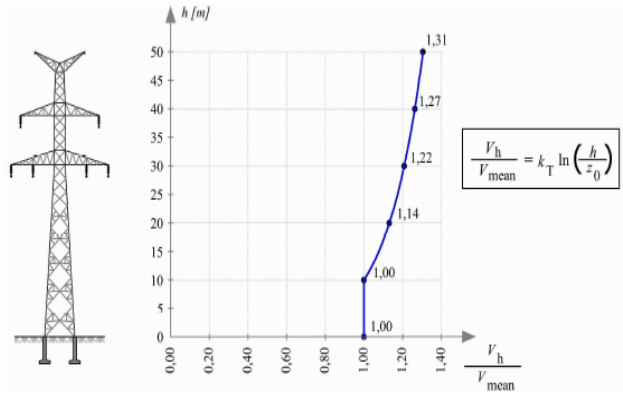


Fig. 14 The relation between the mean value of wind and the wind velocity for each section of the considered tower (Ref. 47)

#### 4.4.2. Probabilistic icing load

Since no ice data was available from field measurements, the values given by Ref. 47 are taken as a reference to model the ice probability. In order to describe the probabilistic icing load, the Weibull random variable is assumed (Eqn. 1).
The aim is to plot a PDF of the corresponding ice thickness in relation to the maximum monthly wind speed. It is said in Ref. 48 that the ice load resulting from icing events usually remains on the conductors for around six days, thus it is conservatively assumed that the maximum monthly wind acts during the freezing event.
The value recommended by Ref. 47 for the coastal regions and lowlands, considering a diameter of 21.7 mm (AFL-6 240 conductor), is the basic ice load of 13 N/m. Thus the diameter of the ice-covered conductor is taken as 48.4 mm. Therefore, the radial thickness of ice cover is equal to 13.4 mm.
According to Ref. 49 the corresponding wind velocity of 10.4 m/s appears during an icing event given the above ice thickness value.
In order to model the icing probability properly some selected assumptions are introduced.
First of all, the icing load is supposed to act at the same time as the maximum monthly wind. This is a safety assumption, because the two maximum monthly events may not be concurrent at the same time, the opposite situation is taken into account in the paper. Nevertheless, as ice might remain in the conductors up to six or even more days, and icing events observed in most countries usually are combined with relevant wind speeds, a set combination of those loads proposed in the paper is justified. Therefore an accuracy loss is expected due to the implementation of this hypothesis, however the loss is not high, from an engineering viewpoint providing enough design safety.
In order to determine the Weibull-type variable shape and scale factors, the ice thickness related to a return period of 50 years is taken equal to the thickness imposed by the standard. The ice thickness resulting from the application of a design load safety factor of 1.5 is related to a return period of 150 years.
The icing event is linked with a probability of occurrence equal to 0.916, which means that only one severe icing storm per year is expected. This is a result of the observations reported by (Refs 48 – 50) in Central Europe.
Taking these assumptions into account, the value of shape parameter equal to $k$ = 0.38 and the scale factor equal to λ = 0.103 for the Weibull distribution given in Eqn. 1 are calculated. The image of the output Weibull probability density function (PDF) is shown in Fig. 15.

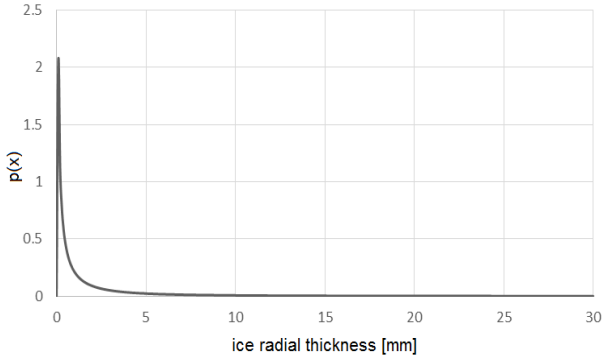


Fig. 15 The Weibull's probability density function of the icing load (in terms of the ice radial thickness on loaded elements)

#### 4.4.3. Structural response definition

The observed structural response *u(x)* was expressed in terms of a critical load value multiplier, calculated for every tower randomly generated model in Simulia ABAQUS/CAE 6.14-2.

### 4.5. Reliability assessment of the tower

According to the studies presented in Ref. 51, the supporting towers are the weakest components of the power transmission lines. Foundations and insulators are supposed to be more reliable than the tower itself, so their impact is not taken into account in the paper.

Thus it is assumed that the reliability of the tower determines the reliability of an entire power grid system.

#### 4.5.1. Wind load return period in reliability calculations

In the design of overhead lines, return periods $T_R$ of climatic loading comprising the interval of 50 – 1000 years are considered. According to Ref. 44 yearly failure probability is between $1/T_R$ and $1/2T_R$, if the ULS scenario assumes that the design strength (90% of the characteristic strength) is considered to be equal to the load effect.
Hence the probability of failure $P_{F,N}$ during a period of $N$ years is given by Eqn. 4:

$$P_{F,N} = 1 - \left(1 - P_{F,1}\right)^N \tag{4}$$

Overhead power lines can be designed considering different levels of reliability, depending on the power provider requirements. Usually three different levels of reliability are assigned depending on the line voltage. Reliability level 1 considers loading conditions according to a 50-year return period, selected for lines up to 150 kV.
Reliability level 2 can be chosen for lines above 230 kV if the line is an important element in the power grid or if it is the only source of electricity. This reliability level considers loading conditions of 150-years return period.
Reliability level 3 using loads of 500-years return period is selected for those lines which interconnects different power grids, deliver power to large amount of consumers, cross important traffic routes and urban areas and connects power plants.
Nevertheless, national standards may specify different reliability levels, in particular Ref. 47 does not specify any reliability target, which means, that due to the planned service life of structures, the 150 and 500 year period are purely hypothetical. In the paper, they are analyzed mainly for comparative purposes.
It should also be taken into account, that although a climatic loading for a given return period is chosen, after applying the safety coefficients for ultimate limit state calculations, the return period will increase. When a climatic load with a return period of 50 years is considered in real-life structural design, applying the standard design safety factor results that in fact, a 500 years return period is considered, the failure probability is made significantly lower due to design values.

#### 4.5.2. ULS climate loads interaction

Once the loading conditions of probabilistic outtake of wind and icing are known, the joint wind-ice interaction is investigated to possibly lead to the tower collapse.
The following assumptions are made: first, the tension of cables is assumed symmetrical, so the ice load is uniformly distributed along the entire neighboring spans, next, structural collapse is assumed to happen for all the weather combinations leading to maximum stresses $\sigma$ such that the Eqn. 5 is fulfilled:

$$\frac{f_y}{\gamma_{M0}} > \sigma > \frac{f_y}{\gamma_{M1}} \rightarrow 355\ \text{MPa} > \sigma > 338\,\text{MPa} \tag{5}$$

where the factors $\gamma_{M0} = 1.0$ and $\gamma_{M1} = 1.05$ are taken according to Ref. 1.
In the case of the analyzed tower the critical combinations of wind and icing loading are shown in Fig. 16.

#### 4.5.3. The choice of probabilistic methods

First of all, a reliability calculation method should be chosen. The initial structural reliability is very high, so the techniques to find an exact Limit State Equation are required.
Like in the previous chapter, the crude Monte Carlo method was the reference method, but also directed variance reduction techniques were suggested. The RSM-based index was also used in the analysis.
Using the inverse transform method for the standardized sample space, for each of the return period scenarios 6000 random samples were generated. A presented calibrated LSF created the possibility of samples calculation independently of the Autodesk ROBOT Structural Analysis Professional 2016 commercial software.

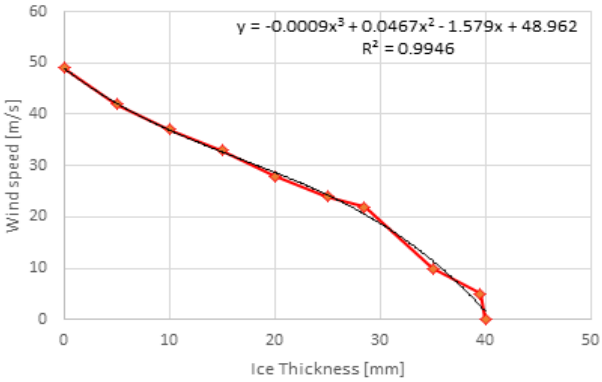


Fig. 16. The Limit State Function (3rd order polynomial approximation equation provided) of possible wind and icing loads – the right hand side depicts the failure region

#### 4.5.4. The 50-year wind speed return period scenario

The results of the Monte Carlo simulation in the 50-year return period scenario are presented in Fig. 17.
In the simulation no samples were generated outside the safe region, thus the probability of failure $P_{F,50years} = 0$. It is worth noting, that this is a similar situation to that displayed in the example in Chapter 3, even although the number of samples is more than 100 times higher. This result also should not be considered accurate, as the number of samples seems to not be satisfactory, even although the mean value and standard deviation convergence were fully achieved. Moreover, there are known cases of similar structures collapse due to atmospheric loads alone, as proved in Refs 52 - 55.

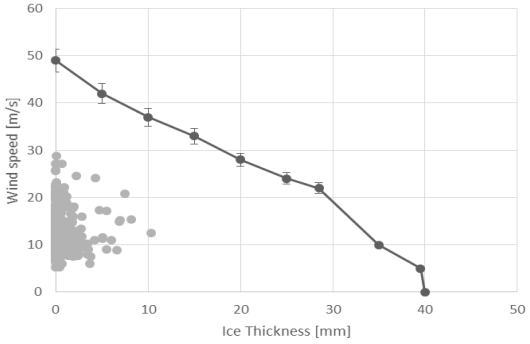


Fig. 17 Monte Carlo simulation in the 50-year return period scenario (6000 random samples analyzed)

In order to improve the quality of this analysis, further MC samples were generated, up to the number of 30,000. However, still no sample beyond the limit state function was generated. The probability of failure was still shown equal to zero.
Such a situation demands a cross-check of the MC result, so the RSM methodology was incorporated. The methodology does not require any additional sample calculation, as it operates well on the previous MC calculations. Due to time consumption the convergence check of the RSM approximation was performed every 100 samples. Considering approximately 500 samples the surface equation detected a full convergence, indicating the Hasofer-Lind-Rackwitz-Fiessler (HLRF) reliability index value equal to $\beta_{HLRF,RSM,50years} = 3.63$ and the equivalent probability of failure equal to $P_{F,RSM,50years} = 0.139\times10^{-3}$. On the other hand, it seems a considerable result, contradict to the MC conclusions. The observation of the response surface fit in the vicinity of the Limit State Equation proves, that the good fit to the cloud of MC points does not contribute to the failure region, so the result should not be treated as trustworthy without comparing to other techniques or methods.
Due to such inconsistency of results obtained for both methods, the Stratified Sampling technique was used, and the sample space was divided to 500×500=250000 subspaces, which made the calculations challenging and time-consuming. Although they presented a result equal to $P_{F,SS,50years} = 0.048\times10^{-3}$, equivalent to $\beta_{C,SS,50years} = 3.88$. Not only

this is the most trustworthy result, but also it legitimates the RSM-based result in engineering practice.

#### 4.5.5. The 150-year wind speed return period scenario

The results of the Monte Carlo simulation in the 150-year return period scenario are given in Fig. 18.

No samples were generated outside the safe region. The basic analysis shows the probability of failure $P_{F,150years} = 0$. On the other hand, while comparing Fig. 17 and Fig. 18 it can be clearly seen, that the scatter of the cloud of samples is much higher, indicating, that the real reliability value is slightly lower than the value corresponding to the 50-years scenario. Of course, the zero-result also should not be considered accurate, the number of samples is not satisfactory again.

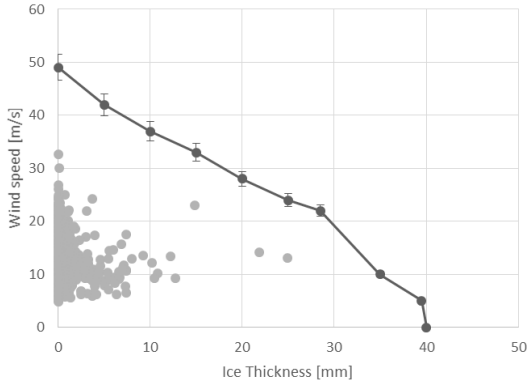


Fig. 18 Monte Carlo simulation in the 150-year return period scenario (6000 random samples analyzed)

Next, the MC analysis was continued with a further MC samples generation, again up to 30,000 samples. Such a magnification of the number of samples has shown two samples in the failure region, so the probability of failure was shown as equal to $P_{F,150years}$ = 2/30,000 = $0.067\times10^{-3}$. This is equal to a reliability index of $\beta_{C,MC,150years} = 3.81$.

It should be noted, that even though the scatter is visibly higher, a smaller failure probability was given than the value of $P_{F,RSM,50years}$ and only a little bigger than the $P_{F,SS,50years}$ value. This may also indicate, that the number of samples in the broadened MC analysis is insufficient and that the probability has a bigger value.

Due to the above mentioned observation, the RSM check was performed again. The RSM approximation was completed after the 500$^{th}$ sample, giving a HLRF reliability index value equal to $\beta_{HLRF,RSM,150years} = 3.38$, equivalent to the probability of failure equal to $P_{F,RSM,150years} = 0.363\times10^{-3}$.

The Stratified Sampling technique was used again, this time the sample space was divided to only 200×200=40000 subspaces. The result of the probability of failure calculations was equal to $P_{F,SS,150years} = 0.175\times10^{-3}$, equivalent to $\beta_{C,SS,150years} = 3.58$. From an engineering viewpoint this result may conclude to accept both results, from the detailed MC method and the RSM.

#### 4.5.6. The 500-year wind speed return period scenario

The Monte Carlo simulation results in the 500-year return period scenario are given in Fig. 19.

In the simulation two samples were generated outside the safe region. The estimated failure probability is $P_{F,500years}$ = 2/6,000 = $0.333\times10^{-3}$, giving the reliability index of $\beta_{C,MC,500years} = 3.40$. Such a result corresponds to the dispersion increase of the MC samples in the sample space of the task.

Despite the sample number increase did not seem necessary, the generation of 30,000 samples was performed for illustrative purposes. The probability of failure was estimated $P_{F,500years}$ = 8/30,000 = $0.267\times10^{-3}$, the corresponding reliability index $\beta_{C,MC,500years} = 3.46$. Both MC results were close, so both variants may be considered trustworthy.

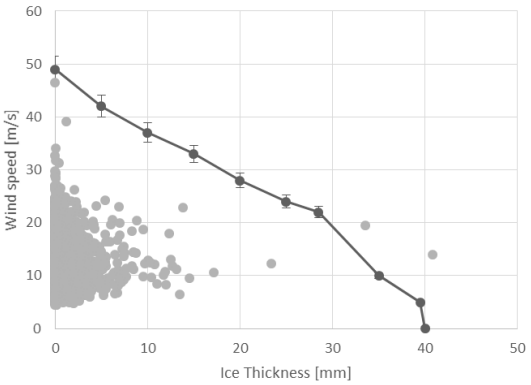


Fig. 19 Monte Carlo simulation in the 500-year return period scenario (6000 random samples analyzed)

Nevertheless, the RSM check was performed and completed after the 500$^{th}$ sample, giving a HLRF reliability index value $\beta_{HLRF,RSM,500years}$ = 3.17, which corresponds to the probability of failure equal to $P_{F,RSM,500years} = 0.777\times10^{-3}$.

It should be noted, that the shift in the cloud of sample shape has made the approximation in the vicinity of the LSF not satisfactory.

The Stratified Sampling technique was performed with 100×100=10000 subspaces. The corresponding probability of failure was $P_{F,SS,500years} = 0.3\times10^{-3}$, equivalent to $\beta_{C,SS,500years} = 3.43$.

#### 4.5.7. The RSM calculations for other wind speed return periods

The RSM calculations, due to their relative simplicity and a small time-consumption were performed also in the case of other wind speed return periods.

Apart from the above results, the 5, 10, 25 and 100 years scenarios were undertaken here to improve the assessment quality.

Failure probabilities obtained in the analysis are shown in Fig. 20. In the figure the $P_F$ values are given, quadratic approximation of the function of $P_F$ change is displayed.

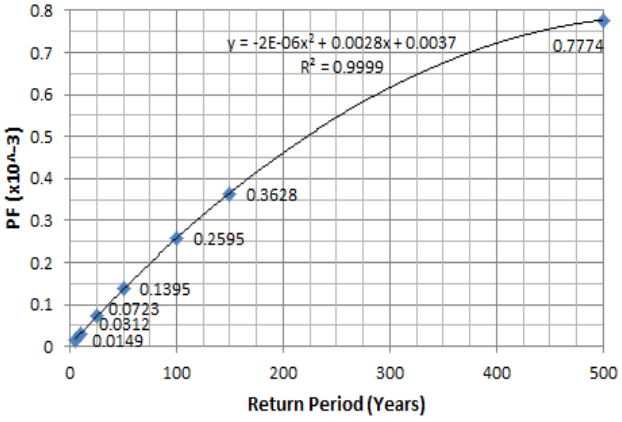


Fig. 20 The probability of failure results obtained using the Response Surface Method for different return periods

### 4.6. Remarks on the example

The results of scenarios lead to an observation that the probabilities of failure with alarming values are restricted to large time periods, longer than 150 years. Taking into account that transmission lines are usually designed for the 50 years' service, thus an extremely low failure probability concerns the studied case.

Taking these results into consideration, high reliability of the tower should be highlighted, this fact may imply that the structure is overdesigned. Nevertheless, some existing design process aspects are necessary to be remarked.

First of all the analyzed tower is aimed to support a cascade failure. This is an accidental load case which has not been taken into account in the reliability assessment, as a strain angle tower, described and analyzed in the paper, is typically not susceptible to this type of failure. An alternative approach, following the same procedure is to estimate reliability of a suspension tower, usually weaker than the strain angle tower, see Ref. 56.
Secondly, even though a specific list of possible extreme load combinations is given in dedicated design codes (Ref. 47), the combinations concerning the possible geometric imperfection occurrence were omitted in the numerical model of the tower.
Regarding the expected failures the icing loading is a decisive factor. No event has been simulated marking the wind alone to trigger tower failure (for $v_{wind} \geq 49$ m/s). Simulations exist showing the ice thickness values $t_{icing} \geq 40$ mm enough to cause the transmission tower collapse regardless of the combined wind intensity.

## 5. CONCLUSIONS

First of all, the analysis presented in the paper allows to formulate a number of comments regarding probabilistic computations.
Consequently, a set of conclusions may be presented concerning the time-induced variability.
Finally, engineering recommendations may be proposed too to facilitate the design process of this class of structures.

### 5.1. Comments on probabilistic computations

Probabilistic structural analysis is a field of engineering subjected to permanent development. Technological progress of numerical methods, combined with a swift development of computer-aided design tools makes it possible to implement probabilistic techniques in engineering processes at the design office level. While parallel solution is possible of a large number of variants of a given structural model in a short time, without the use of high computing power, repetitive computational routine, e.g. the direct Monte Carlo method proves successful. Thus it is possible to more accurately assess the uncertainty impact on structural response, contrary to the standard-based approach regarding all uncertainties by means of resistance and load factors.
No necessity occurs to analyze complicated multivariate problems in the course of structural analysis and design. The results obtained in the paper clearly confirm that proper reduction of the problem size (number of random variables) leads to a significant reduction in computational effort and time consumption. The results of the simplified probabilistic models take the advantage of the solution of a full, complex problem.
Sensitivity analysis is helpful in determining key variables of a given problem. Moreover, an additional impact check of combined change of key variables leads to sensitivity coefficients using the result interval technique, presented in the paper. It allows to identify the elements to be strengthened over time and provides information on the extent of the required remedial actions. It also helps to properly implement the numerical model of a lightweight structure or its element, as shown in Ref. 57.
It has also been shown that the choice of the technique of structural safety measures is important in equal extent to choosing relevant basic random variables.
In the presented numerical examples the crude Monte Carlo method is proved ineffective. Although it is considered a reference method, the required number of realizations is much larger than indicated by statistical moment convergence. In both examples an insufficient number of samples leads to wrong structural reliability assessment.
On the other hand, the variance reduction techniques, e.g. Stratified Sampling or Targeted Random Sampling techniques used in the work fit the abovementioned problem well. However, while these techniques need a new set of samples to be calculated, in order to function properly, the crude Monte Carlo samples cannot be re-used in these techniques. The Stratified Sampling technique requires a high sample population, comparable to the range of the Monte Carlo method for the more accurate structural safety measures determination. The Targeted Random Sampling technique requires a significantly lower sample number, but its algorithm, difficult to implement, requires complex dedicated procedures.
The Response Surface Method (RSM) is intended to be an optimal tool. As the Monte Carlo method data can be re-used in the method, it does not require any new calculations. Moreover, its possible parallel application to the crude Monte Carlo reliability assessment provides a double check of reliability indices. The response surface convergence is fast, the results are easy to interpret. However, it should be ensured that the method is properly balanced between the samples collected in the safe domain and the samples taken from the vicinity of the Limit State Equation. It is believed, although not checked in the considered examples, that the response surface approximation by a combined set of crude Monte Carlo and Targeted Random Sampling points may be optimal in the considered case.

### 5.2. Comments on the variability of random parameters over time

It was shown that stochastic processes may be illustrated as a series of single states in selected time periods. This operation does not bring a significant loss in computational quality. The analysis of several states (time steps) results in a good overview of structural uncertainty and reliability assessment, moreover, it allows to cover structural variation by means of a certain order function. It should be clearly stated, that in most cases such a variation is strongly non-linear.
The time-dependent degradation of material mechanical properties can be expressed by Young's modulus variation (verified by experimental analysis), as shown in Ref. 42 or by the change of cross-sectional areas of structural elements (verified by means of real-life survey of a deteriorated structure), this issue was presented earlier by the Author of Ref. 39. The return period of an exceptional load can be expressed by means of an appropriate parameter modification of probability density function of the considered load.

### 5.3. The recommendations for civil engineers

Both lightweight structures analyzed in the paper are key elements of the system of their installation, mainly due to their structural dimensioning. On the basis of the performed numerical computations it was shown that the submerged structure is the weakest element of the wind power plant (failure always occurs in the submerged segments), and the transmission tower is the weakest element of the electric grid (failure of an entire grid occurs while the cross-arms or the curbs of the tower fail). Thus a need is strongly suggested for a thorough probabilistic analysis of such structures.
It is believed that the duty of the structural designer is not limited only to the initial state analysis of the structure (the design state) but should be extended to all vital operating conditions of the structure at the end of its planned service time (the degraded state).
The data regarding the factor-based design provided in the standards may not be sufficient if there is no adequate protection or maintenance of a structure during its planned period of operation.
It is highly recommended to take a step towards an engineering process based on probabilistic design codes. The JCSS probabilistic model code (Ref. 2) should be pursued, presenting random nature of loads compatible with the worldwide load database. In the operational time of a new code format it has been subjected to a successful cross-check with the factor-based design procedures, applied in the design of currently operating lightweight structures.

## REFERENCES


1. PN-EN 1991-1-1. Actions on structures.
2. Vrouwenvelder, T. (1997). The JCSS probabilistic model code. Structural Safety, 19(3), 1997, pp. 245–251.
3. ISO 2394:2015. General principles on reliability for structures.
4. Elishakoff I.: Probabilistic methods in the theory of structures. John Wiley and Sons, Chichester 1983.
5. Rackwitz R., Fiessler B.: Structural reliability under combined random load sequences. Computers and Structures, 9, 1978, pp. 489–494.
6. Thoft–Christensen P., Baker M.J.: Structural Reliability Theory and Its Applications. Springer-Verlag, Berlin, 1982.

7. Freudenthal A.M.: Safety and the probability of structure failure. Journal of Engineering Mechanics, Transitions of American Society of Civil Engineers, 121, 1956, pp. 1337.
8. Lin Y.K.: Probabilistic Theory of Structural Dynamics. McGraw-Hill, New York, 1967.
9. Haugen E.B.: Probabilistic approach to design. John Wiley and Sons, Chichester, 1968.
10. Cornell, C.A.: A Probability-Based Structural Code. American Concrete Institute Journal, 66, 1969, pp. 974–985.
11. Lind N.C.: Structural reliability and codified design. University of Waterloo, Waterloo, 1970.
12. Hasofer A.M., Lind N.C.: An Exact and Invariant First-Order Reliability Format. American Society of Civil Engineers Journal of Engineering Mechanics Division, 100, 1974, pp. 111–121.
13. Lind N.C.: Formulation of probabilistic design. American Society of Civil Engineers Journal of Engineering Mechanics Division, 103, 1977, pp. 273–284.
14. Ditlevsen O.: Uncertainty Modelling. McGraw-Hill, New York, 1981.
15. Vanmarcke E.-H.: Random Fields: Analysis and Synthesis. MIT Press, Cambridge, 1983.
16. Madsen H.O., Krenk S., Lind N.C.: Methods of Structural Safety. Prentice-Hall, New Jersey, 1986.
17. Hohenbichler M., Gollwitzer S., Kruse W., Rackwitz R.: A new light on first and second order reliability methods, Structural Safety, 4(4), 1987, pp. 267–284.
18. Melchers R.E.: Structural Reliability Analysis and Prediction. John Wiley and Sons, Chichester, 1999.
19. Sudret B., Der Kiureghian A.: Stochastic Finite Element Methods and Reliability. A State-of-the-Art Report. Department of Civil and Environmental Engineering, University of California, Berkeley, 2000.
20. Ang A.H-S., Tang W.H.: Probability Concepts in Engineering. Emphasis on Applications in Civil and Environmental Engineering. John Wiley and Sons, London, 2007.
21. Kahn H.: Use of different Monte Carlo sampling techniques. Proceedings of the Symposium on Monte Carlo Methods, John Wiley and Sons, New York, 1956, pp. 149–190.
22. Hammersley J.M., Handscomb D.C.: Monte Carlo Methods. Fletcher & Son Limited, Norwich, 1964.
23. Pradlwarter H.J., Schuëller G.I.: On advanced Monte Carlo simulation procedures in stochastic structural dynamics. International Journal of Non-Linear Mechanics, 32, 1997, pp. 735–744.
24. Hurtado J.E., Barbat A.H.: Monte Carlo techniques in computational stochastic mechanics. Archives of Computational Methods in Engineering, 5, 1998, pp. 3–30.
25. Johnson E.A., Bergman L.A., Spencer Jr B.F.: Intelligent Monte Carlo simulation and discrepancy sensitivity. Computational Stochastic Mechanics, 1, 1999, pp. 31–39.
26. Schuëller G.: Computational stochastic mechanics – recent advances. Computers and Structures, 79, 2001, pp. 2225–2234.
27. Hong, H.P.: An efficient point estimate method for probabilistic analysis, Reliability Engineering and System Safety, 59(3), 1989, pp. 261–267.
28. Ditlevsen O.: Model uncertainty in structural reliability. Structural Safety, 1, 1982, pp. 73–86.
29. Chen X., Lind N.C.: Fast probability integration by three-parameter normal tail approximation. Structural Safety, 1, 1983, pp. 269–276.
30. Ditlevsen O., Madsen H.O.: Structural reliability methods. John Wiley and Sons, Chichester, 1996.
31. Kamiński M.M.: The Stochastic Perturbation Method for Computational Mechanics. John Wiley & Sons, London, 2013.
32. Myers R.H., Montgomery D.C.: Response Surface Methodology: Process and Product Optimization Using Designed Experiments. John Wiley and Sons, New York, 1995.
33. Khuri A.I., Cornell J.A.: Response Surfaces. Dekker, New York, 1996.
34. Shinozuka M., Yamazaki F.: Stochastic finite element analysis, an introduction. Stochastic Structural Dynamics. Elsevier Science, Amsterdam, 1988, pp. 241–291.
35. Cheng A.H.-D., Young C.Y.: Computational stochastic mechanics. Elsevier, London, 1993.
36. Grigoriu M.: Stochastic Mechanics. International Journal of Solids and Structures, 37, 1999, pp. 197–214.
37. Wei K., Arwade S.R., Myers A.T.: Incremental wind-wave analysis of the structural capacity of offshore wind turbine support structures under extreme loading. Engineering Structures, 79, 2014, pp. 58–69.
38. Ptaszek R., Górski J., Winkelmann K.: The impact of material degradation on the resistance and reliability of truss structures. Lightweight Structures in Civil Engineering–Contemporary Problems Conference Proceedings, Olsztyn, 2016, pp. 77–80.
39. Winkelmann K., Bosch J.L., Górski J.: Structural reliability of overhead power lines by means of Monte Carlo Method and RSM, 3rd Polish Congress of Mechanics and 21st International Conference on Computer Methods in Mechanics, PCM-CMM-2015 Conference Proceedings, Gdańsk, 2015, pp.747–748.
40. Morison J. R.: The Force Distribution Exerted by Surface Waves on Piles. University of California Technical Report Series, 3, 345, 1953, pp. 1–3.
41. Weibull W.: A Statistical Theory of Strength of Materials. Ingeniör Vetenskaps Akademin Proceedings, Stockholm, 1939.
42. Song H.W., Pack S.W., Ann K.Y.: Probabilistic assessment to predict the time to corrosion of steel in reinforced concrete tunnel box exposed to sea water. Construction and Building Materials, 23, 2009, pp. 3270–3278.
43. DNV-OS-C101:2011. Offshore Standard: Design of offshore steel structures, general LRFD method.
44. Kissling E., Nefzger P., Nolasco J.F., Kainzyk V.: Overhead Power Lines. Planning, Design, Construction, Springer-Verlag, Heidelberg, 2003.
45. Gumbel E.J.: The return period of flood flows. The Annals of Mathematical Statistics, 12, 1941, pp. 163–190.
46. Palutikof J.P., Brabson B.B., Lister D.H., Adcock S.T.: A Review of Methods to Calculate Extreme Winds. Meteorological Applications, 6, 1999, pp. 119–132.
47. PN-EN 50341-1:2013-03. Elektroenergetyczne linie napowietrzne prądu przemiennego powyżej 1 kV. Część 1: Wymagania ogólne. Specyfikacje wspólne.
48. Farzaneh M.: Atmospheric icing of power networks. Springer, Berlin, 2008.
49. Fikke S., Ronsten G., Heimo A., Kunz S., Ostrozlik M., Persson P.E., Sabata J., Wareing B., Wichura B., Chum J., Laakso T., Säntti K., Makkonen L.: COST 727: Atmospheric Icing on Structures Measurements and data collection on icing: State of the Art. Publication of MeteoSwiss, Zurich, 2006.
50. Simiu E., Heckert N.A., Filliben J.J., Johnson S.K.: Extreme wind load estimates based on Gumbel distribution of dynamic pressures: an assessment. Structural Safety, 23, 3, 2001, pp. 221–229.
51. Mendera Z., Wandzik G.: Design of Truss Towers for Overhead Power Lines (in polish), Katowice, 2012.
52. Brostörm E.: Ice Storm Modelling in Transmission System Reliability Calculations, KTH, Stockholm, 2007.

53. Dymek D., Jastrzębska E., Kurbiel W.: Failures of OVH power lines caused by icing. Szczecin, 2013.
54. Lamraoui F., Fortin G., Benoit R., Perron J., Masson C. Atmospheric icing severity: Quantification and mapping. Atmospheric Research, 128, 2013, p. 57–75.
55. Jones K., Thorkildson R., Lott N.: The Development of United States Climatology of Extreme Ice Loads. National Climatic Data Center. Technical Report, New York, 2002.
56. Yang Q., Xiong X., Wei Y., Wang J., Weng S.: Short-Term Reliability Evaluation of Transmission System under Strong Wind and Rain. Journal of Power and Energy Engineering, 2, 2014, pp. 665–672.
57. Mikulski T., Kujawa M., Szymczak C.: Problems of analysis of thin-walled structures. Statics, free vibrations and sensitivity. Proceedings of European Congress on Computational Methods in Applied Sciences and Engineering (ECCOMAS 2012), Vienna, 2012, pp. 1–19.